https://doi.org/10.5194/essd-2021-61
Preprint. Discussion started: 16 March 2021

Open Access Earth System Science Data Discussions

A Harmonized Global Land Evaporation Dataset from Reanalysis Products Covering 1980-2017

Jiao Lu[1], Guojie Wang[1]*, Tiexi Chen[1], Shijie Li[1], Daniel Fiifi Tawia Hagan[1], Giri Kattel[1], Jian Peng[2,3], Tong Jiang[1], Buda Su[1]

[1]Collaborative Innovation Center on Forecast and Evaluation of Meteorological Disasters, School of Geographical Sciences, Nanjing University of Information Science & Technology, Nanjing 210044, China
[2]Department of Remote Sensing, Helmholtz Centre for Environmental Research - UFZ, Permoserstrasse 15, 04318, Leipzig, Germany
[3]Remote Sensing Centre for Earth System Research, Leipzig University, Talstr. 35, 04103, Leipzig, Germany

Correspondence to: Guojie Wang (gwang@nuist.edu.cn)

Abstract. Land evaporation (ET) plays a crucial role in hydrological and energy cycle. However, the widely used numerical products are still subject to great uncertainties due to imperfect model parameterizations and forcing data. Lack of available observed data has further complicated the estimation. Hence, there is an urgency to define the global benchmark land ET for climate-induced hydrology and energy change. In this study, we have used the coefficient of variation (CV) and carefully selected merging regions with high consistency of multiple data sets. Reliability Ensemble Averaging (REA) method has been used to generate a long-term (1980-2017) daily ET product with a spatial resolution of 0.25 degree by merging the selected three data sets, ERA5, GLDAS2 and MERRA2. GLEAM3.2a and flux tower observation data have been selected as the data for reference and evaluation, respectively. The results showed that the merged product performed well under a variety of vegetation cover conditions as the weights were distributed across the east-west direction banding manner, with greater differences near the equator. The merged product also captured well the trend of land evaporation over different areas, showing the significant decreasing trend in Amazon plain in South America and Congo Basin in central Africa, and the increasing trend in the east of North America, west of Europe, south of Asia and north of Oceania. In addition to model performance, REA method also successfully worked for the model convergence showing as an outstanding reference for data merging of other variables. Data can be accessed at https://doi.org/10.5281/zenodo.4595941 (Lu et al., 2021).

1 Introduction

Land evaporation plays an important role in the exchange of energy, water and carbon in the terrestrial biosphere, hydrosphere and atmosphere. It is one of the dominant components of land water and energy budget, as well as a key driver of drought episode (Seneviratne, 2012; Sheffield et al., 2012). Therefore, it is important to quantify the spatial and temporal patterns of land evaporation. In addition, it is used to estimate water requirements for irrigation by agricultural and water resource management groups. The strength of the hydrological cycle determines water availability and affects the climate system in a variety of ways (Mueller et al., 2013). Apart from hydrological applications, land evaporation change is also

https://doi.org/10.5194/essd-2021-61
Preprint. Discussion started: 16 March 2021


Open Access Earth System Science Data Discussions

related to air temperature change and extreme high temperature condition (Seneviratne et al., 2006, 2010; Hirschi et al., 2011; Mueller and Seneviratne, 2012). It is apparent that land evaporation is regarded as the intermediate variable of soil moisture affecting air temperature. To summarize, the uncertainty of land evaporation estimation will introduce adverse errors in various aspects, which puts the global benchmark ET data set in a crucial position.

Since land surface is more heterogeneous than the ocean, it is difficult to estimate land evaporation accurately due to huge uncertainties resulted from complex land-atmosphere feedback processes. In addition, a major challenge remains to be addressed, for instance, there is no direct signal describing land evaporation that has been remotely detected. However, satellite observations relating to surface temperature, soil moisture or vegetation coverage data can be combined with traditional flux formulas as an alternative method to derive global estimates at different temporal and spatial scales (Monteith, 1965; Priestley and Taylor, 1972). In recent years, multiple land evaporation data sets at global scales are also available from in situ observations and satellite inversion. The available terrestrial ET datasets have widely varying estimates and even opposite long-term trends, indicating the existence of non-negligible uncertainties. Further, satellite-based land evaporation products show great discrepancies when compared with latent heat flux from flux towers (Jimenez et al., 2011; Mueller et al., 2011; McCabe et al., 2016; Peng et al., 2016, 2020). Although the latent heat flux is widely used as the benchmark for assessing the quality of land ET data sets, flux tower is unevenly distributed around the world, only densely in some regions of North America, Europe and Oceania (as shown in Fig. 1). As a result, a benchmark for global land ET is still needed, in spite of large number of land evaporation data sets available for research and analysis. On account of these reasons, a land ET benchmark synthesis product was developed based on currently widely used data sets to reduce the uncertainties of land ET in this study.

In previous studies, far from hindering the use of these land evaporation data sets, differences among the products are capable of facilitating researches for the best merging methods to obtain data sets with lower uncertainties (Jimenez et al., 2018). Due to differences in the algorithm and the calibration coefficient, the simulated results would have greater discrepancies. The land evaporation with relatively high precision has been achieved when various methods are combined. Although this may not necessarily lead to better prediction ability of land evaporation and increased understanding of physical processes, uncertainties can be reduced by the integration of multiple remote sensing products (Jung et al., 2010; Mueller et al., 2013) and more complex data merging methods (Yao et al., 2014).

The effectiveness of hydrometeorological monitoring can be improved by accurate quantification and further reduction of the uncertainty of water cycle variables especially land ET. Therefore, a variety of merging techniques have been introduced and applied to water cycle variables such as soil moisture and precipitation in recent years. Least-squares (Yilmaz et al., 2012) and maximization R (Kim et al., 2015, 2018) techniques were proposed for satellite soil moisture products merging. However, the practical application of maximized R method is usually found limited due to its use of only two most relevant in given data sources. In regard to precipitation data merging, geographically weighted regression algorithm (Xu et al., 2015), conditional merging (Baik et al., 2016), geographical difference analysis (Cheema and Bastiaanssen, 2012) and geographic

https://doi.org/10.5194/essd-2021-61
Preprint. Discussion started: 16 March 2021

ratio analysis (Duan and Bastiaanssen, 2013) have been widely used. As for land ET, several relevant studies have evolved through simple average to complex methods including the weighted average (Hobeichi et al., 2018), reproducing flux observations combined with the original land evaporation product (Yao et al., 2017a), or seeking consistency between land evaporation and water cycle related products such as precipitation, runoff and land water storage (Aires et al., 2014; Munier et al., 2014). Diversified data merging methods, such as Kalman filtering algorithm (Pipunic et al., 2008; Liu C et al., 2013), Bayesian Model Average (BMA) and Empirical Orthogonal Function (EOF), can improve regional ET estimation by merging multiple ET products (Yao et al., 2014, 2016; Feng et al., 2016; Zhu et al., 2016). Since land ET is a complex variable coupling energy, hydrology and carbon budget, it is difficult to accurately determine the conditional density in BMA. In addition, EOF not only requires high computational cost, but also introduces bias due to the lack of distinction between good and bad quality Pixel in the refactoring scheme. Simultaneously, their complexity affects the efficiency of calculating the weight of individual data set, which limits their wide application. Simple average (SA) (Ershadi et al., 2014) and simple Taylor skill's score (STS) merging (Yao et al., 2017b) have been adopted for global ET merging. However, SA assumes the same uncertainty in each data set, which is actually unreasonable, and STS is highly dependent on the accuracy of single data, which makes it highly quality-demanding for the data sets involved in the merging process. Khan et al. (2018) analyzed the sources of uncertainties for three different ET products using triple collocation (TC) method, which estimates the random error standard deviations for three datasets of the same variable according to statistical relations, and provides an uncorrelated absolute and relative error structure among data sets. It has a strict requirement for the number of data sets participating in the merging process, which affects the flexibility of data merging greatly. Lately, Jimenez et al. (2018) proposed an error variance unweighted merging method with the local weights deduced according to the variance of the differences between the outliers of the flux tower and simulated land evaporation. The above merging methods effectively reduce the uncertainties of simulations by estimating the weight of multiple products to generate reliable merged products (Zhu et al., 2016). However, previous studies have mostly focused on the evaluation of ET simulation at regional scales and landscape (Yang et al., 2016).

Compared to the simple method, Reliability Ensemble Average method (REA) extracts the most reliable information from each model by minimizing the impact of "outliers" or underperforming models, subsequently reducing the uncertainty range in simulated changes, which also stands out in terms of computational efficiency. These standards are regional rather than global, as most models tend to show anomalous behavior or poor performance from one region to another. The REA method also produces a quantitative measure of reliability, which increases the overall reliability of simulation changes. On one hand, REA method considers model performance, that is, the ability of models reproducing current climate, which is defined by the difference between the simulation and observation. On the other hand, the model convergence, a factor to measure the reliability of the modes is taken into consideration as well. It is the distance between the changes of the given model and that of REA average. REA has been widely used for meteorological variables such as precipitation and temperature. Giorgi & Mearns (2002) used the REA to integrate the average seasonal temperature and precipitation of 22 land regions in the world

https://doi.org/10.5194/essd-2021-61
Preprint. Discussion started: 16 March 2021

under two emission scenarios simulated by 9 atmosphere-ocean circulation models in the late 21st century. However, studies on the application of land evaporation are few. This study aims to develop a long-term high-quality global land ET using merging technology. Merging multiple single data sets is expected to reduce the uncertainties of land ET effectively. The merged product can provide a basis for water cycle research and global water resources management. Hence, the systematic and in-depth studies on land evaporation merging are urgently needed.

2 Data and methods

2.1 Data types

Four widely used land ET data sets were selected for merging, including Global Land Evaporation Amsterdam Model (GLEAM; Miralles et al., 2011), the fifth-generation ECMWF Re-Analysis (ERA5; Hersbach et al., 2020), the second Modern-Era Retrospective analysis for Research and Applications (MERRA2; Gelaro et al., 2017), and Global Land Data Assimilation System ET (GLDAS; Sheffield & Wood, 2007). The differences in spatial and temporal resolution among the ET products were rescaled to a daily timescale and 0.25°, with the time span from 1980 to 2017. GLEAM was used as the reference data due to its independence from other data sets participating in the merging process. The data involved in merging includes ERA5, MERRA2 and GLDAS. Eddy Covariance (EC) ET was used to evaluate the merged product compared with other data sets involved in the merging process. The spatial and temporal resolutions of these ET datasets are shown in Table 1, which is briefly described below.

Table 1. Summary of ET data sets involved in merging.

Name	ET schemes/ land-surface schemes	Spatial resolution (degree)	Temporal resolution	Time span	Reference
GLEAM3.2a	Priestley-Taylor	0.25×0.25	daily	1980-2017	Miralles et al. (2011)
ERA5	IFS	0.25×0.25	1-hour	1980-2017	Hersbach et al. (2020)
MERRA2	GEOS-5	0.625×0.5	daily	1980-2017	Gelaro et al. (2017)
GLDAS2.0 & 2.1	Noah	0.25×0.25	3-hour	1980-1999& 2000-2017	Sheffield & Wood (2007)

https://doi.org/10.5194/essd-2021-61
Preprint. Discussion started: 16 March 2021

115 **2.1.1 Global Land Evaporation Amsterdam Model (GLEAM) ET**

GLEAM algorithm estimates land evaporation mainly based on the parameterized physical process, which uses extensive independent remote sensing observations as the basis for calculating land evaporation and its different components including transpiration, bare-soil evaporation, interception loss, open-water evaporation and sublimation separately (Priestley and Taylor, 1972). The empirical parameters contained in this algorithm have been obtained from the findings in different fields.
120 On a global scale, GLEAM has been validated with the observations obtained from the eddy covariance instrument, indicating that it can be used to describe terrestrial ET in different ecosystems (Miralles et al., 2011). The version of the data set used in this study is 3.2a, which spans a 38-year period through 1980 to 2017, gridded with 0.25 degree. It is available from https://www.gleam.eu/.

2.1.2 The fifth-generation ECMWF Re-Analysis (ERA5) ET

125 Followed by ERA-15, ERA-40 and ERA-Interim, the fifth generation of ECMWF reanalysis data ERA5 has been released, which is envisioned to replace ERA-Interim reanalysis (Hersbach et al., 2020). Compared with ERA-Interim, some of the key climatic information of the EAR5 has been improved. The most updated version of the Earth System Model and data assimilation techniques used at ECMWF have been applied in ERA5, including more sophisticated parametrization of geophysical processes in comparison to the previous versions used in ERA-Interim. ERA5 covers from 1979 to the near real
130 time period (on a regular basis), moreover, temporal and spatial resolution have been improved in ERA5, from 6-hourly in ERA-Interim to hourly, from 79 km to 31 km in the horizontal dimension and 60 to 137 in vertical levels. ERA5 has a better balance of global precipitation and evaporation (Albergel et al., 2018). It is available from https://www.ecmwf.int/en/forecasts/datasets/reanalysis-datasets/era5/.

2.1.3 The second Modern-Era Retrospective analysis for Research and Applications (MERRA2) ET

135 MERRA2 (Gelaro et al., 2017) is an advanced atmospheric reanalysis data set, which absorbs mass of satellite data, including the new observation types such as hyperspectral radiation, microwave and aerosols. The MERRA2 is unique in modern reanalysis data set that contains aerosol data assimilation (Randles et al. 2017). It combines satellite and more traditional weather observations with simulated atmospheric behavior, making an attempt to get the optimal possible estimation of the Earth system state. MERRA2 is the second version of MERRA, which has undergone several major
140 upgrades, including an observation-based precipitation bias correction (Reichle et al., 2017). The land surface model used in MERRA2 is the Catchment Land Surface Model (Koster et al., 2000), where land evaporation is calculated as part of the energy balance at the land surface. Hourly data with a 0.625× 0.5° spatial resolution are provided by the Goddard Earth Sciences Data and Information Service Center (DISC). Daily data from 1980 to 2017 has been used in this study. Monthly outputs of simulated surface latent heat fluxes and precipitation have been assessed. The accuracy of MERRA2 has been

https://doi.org/10.5194/essd-2021-61
Preprint. Discussion started: 16 March 2021

widely evaluated (Bosilovich et al., 2015; Gelaro et al., 2017). It is available from https://goldsmr4.gesdisc.eosdis.nasa.gov/data/MERRA2/M2T1NXLND.5.12.4/.

2.1.4 Global Land Data Assimilation System ET (GLDAS) ET

GLDAS is a global high-resolution land modeling System based on North American Land Data Assimilation System (NLDAS), which combines data assimilation technology to produce land surface state and fluxes in real time. In order to generate better land surface products in different LSM, GLDAS generates the optimal field of surface state and flux by absorbing satellite and surface observation data, taking advantage of advanced land surface modeling and data assimilation technology (Rodell et al., 2004). Different LSMs were used including Mosaic, Noah, CLM, and VIC, where only Noah has continued until now. Recently, there is more and more evidence to show that GLDAS-1.0 has serious discontinuities due to forcing data such as large precipitation and temperature errors in 1996 and 2000-2005 (Wang et al., 2016). Therefore, monthly land evaporation data of GLDAS2 combined with Noah LSM (GLDAS2-Noah) has been used in this study, whose spatial resolution is 0.25°×0.25°. GLDAS2 includes two data sets, specifically GLDAS-2.0 and GLDAS-2.1 where the simulations start from 1948 in GLDAS-2.0 and 2000 in GLDAS-2.1. The product is simulated with the Princeton University meteorological forcing data set (PUMFD), which has been corrected with observation-based products during the period of 1948-2010 (Sheffifield et al., 2006). Time period of GLDAS-2.0 from 1980 to 1999 and GLDAS-2.1 from 2000 to 2017 are selected in this study. Details of forcing data and description of the model are available on http://disc.Sci.GSFC.NASA.Gov/Hydrology. They are available from https://hydro1.gesdisc.eosdis.nasa.gov/data/GLDAS/GLDAS_NOAH025_3H.2.0/ and https://hydro1.gesdisc.eosdis.nasa.gov/data/GLDAS/GLDAS_NOAH025_3H.2.1/.

2.1.5 Eddy Covariance (EC) ET

Latent heat flux (LE) from 182 effective flux towers across the world is used to evaluate the performance of multiple data sets with different estimates, which are available from http://fluxnet.fluxdata.org/. Eddy covariance is a widely used energy flux measurement method that provides continuous measurement of interchange of water and energy (Mu et al., 2011). The period of latent heat flux is 1 to 19 years, where 2 to three 3 are the most common, shown in Fig. 1. The observed land evaporation is calculated by latent heat flux in the following Eq. (1),

$$ET = \frac{LE}{\lambda}, \quad (1)$$

where λ is the conversion factor with the fixed value of 2.45MJ kg^{-1}. The flux towers are located in ten land cover types including Croplands (CRO), Deciduous Broadleaf Forest (DBF), Evergreen Broadleaf Forest (EBF), Evergreen Needleleaf Forest (ENF), Grasslands (GRA), Mixed Forest (MF), Open Shrublands (OSH), Savannas (SAV), Permanent Wetlands (WET) and Woody Savannas (WSA).

https://doi.org/10.5194/essd-2021-61
Preprint. Discussion started: 16 March 2021

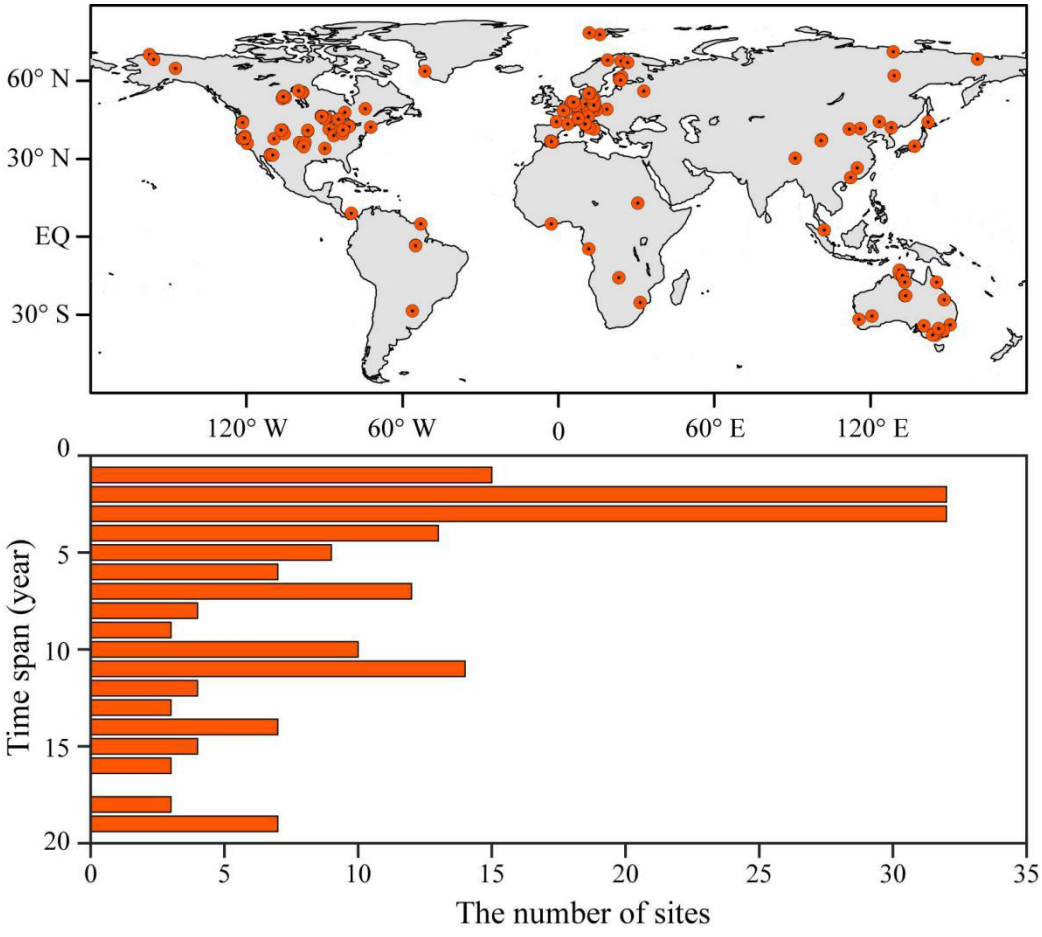

175 **Figure 1. Spatial distribution of 182 in-situ flux EC sites across the world and the number of sites for different time span.**

2.2 Methods

In this study, we investigated whether more accurate ET results could be obtained through the weighted combination of ERA5, GLDAS and MERRA2 estimation. Ideally, the weight assigned to each product should be based on an accurate description of the uncertainty during the merging process. Therefore, three data sets have been weighted based on GLEAM,
180 and the performance of the merged ET products have been studied at the selected sites. A set of weights need to be defined for weighted combination of three products, usually based on an individual uncertainty of each product. The simplest strategy used in previous studies is to assume that all three products have the same uncertainty, thus the merged product is a simple average of each product. A more detailed strategy used in this study is to weigh the product based on their uncertainties. The expected goal is to develop a product that minimizes Root Mean Square Deviation (RMSD) and
185 maximizes correlation with tower ET, which we call optimal in the context of our merging strategy.

https://doi.org/10.5194/essd-2021-61
Preprint. Discussion started: 16 March 2021

2.2.1 Variable Coefficient

The coefficient of variation (CV), also known as the relative standard deviation in probability theory and statistics, was used to evaluate the consistency of multiple sets of reanalysis ET data. It is a statistic to measure the degree of variation in the data. The consistency decreases with the increase of CV. It is calculated from the following equation:

$$CV = \frac{S}{\overline{x}} \times 100\%, \tag{2}$$

where S represents the standard deviation and $\overline{x}$ represents the average of multiple sets of reanalysis ET data in each pixel.

This approach is superior to standard deviation in evaluating consistency, which can eliminate the influence of different units and/or average on the degree of variation of two or more data. In this paper, multiple sets of reanalysis land evaporation data are blended into a single product based on their performance and convergence criteria.

2.2.2 Reliability Ensemble Averaging

Reliability Ensemble Averaging (REA) method (Giorgi and Mearns, 2002; Xu et al., 2010) were used to combine multiple sets of reanalysis ET data into a single product. Two reliability criteria were considered in the method: model performance and model convergence, in other words, the model's performance in reproducing the current climate and the convergence of simulated values between models.

In our REA method, the average ET is given by a weighted average of all the ensemble members.

$$\widetilde{ET} = \tilde{A}(ET) = \frac{\sum_i R_i ET_i}{\sum_i R_i}, \tag{3}$$

where $\tilde{A}$ represents the REA averaging and R_i represents the model reliability factor defined as:

$$\begin{aligned} R_i &= \left[(R_{B,i})^m \times (R_{D,i})^n \right]^{[1/(m \times n)]} \\ &= \left\{ \left[\frac{\varepsilon_{ET}}{abs(B_{ET,i})} \right]^m \left[\frac{\varepsilon_{ET}}{abs(D_{ET,i})} \right]^n \right\}^{[1/(m \times n)]}, \end{aligned} \tag{4}$$

The merging is extended to pixels rather than just flux tower level, based on the selection of independent GLEAM as reference to compensate for the limited EC measured ET. $R_{B,i}$ and $R_{D,i}$ in Eq. (4) is a measure of the model performance and convergence criteria respectively. $R_{B,i}$ is a factor to measure the reliability of the model through the bias ($B_{ET,i}$) between the simulated ET and the reference, that is, the larger the bias the lower the reliability of the model. $R_{D,i}$ is a factor to measure the reliability in the aspect of the distance ($D_{ET,i}$) between the simulated ET and the ensemble average, that is, the higher the distance the lower the reliability of the model.

https://doi.org/10.5194/essd-2021-61
Preprint. Discussion started: 16 March 2021

The parameters m and n in Eq. (4) are used to measure the relative importance of the two criteria. In this work, assuming the importance of the two criteria is equal, m and n were assigned with 1. However, if the two criteria are given different weights, they may be different. The parameter ϵ in Eq. (4) is a measure of natural variability in 38-yr ET. In order to calculate ϵ, we estimated moving averages after linearly detrending the 38-yr time series data in each pixel. Then, the differences between maximum and minimum of the moving averages are computed as ϵ. In addition, when B and D is less than ϵ, R_B and R_D are set to 1 respectively. In essence, Eq. (4) indicates that the model is reliable when the bias and the distance from the ensemble average are within the limits of natural variability, where RB=RD=R=1. With the bias or distance growing, the reliability of a given model decreases.

2.2.3 Validation Criteria

The error metrics of Pearson correlation coefficient (R), root mean square deviation (RMSD) and unbiased root-mean-square deviation (ubRMSD) were used to verify the blending product. The statistic values are defined as follows:

$$R = \frac{\sum_{i=1}^{n}(M_i - \bar{M})(ref_i - \overline{ref})}{\sqrt{\sum_{i=1}^{n}(M_i - \bar{M})^2}\sqrt{\sum_{i=1}^{n}(ref_i - \overline{ref})^2}}, \quad (5)$$

$$RMSD = \sqrt{n^{-1}\sum_{i=1}^{n}(M_i - ref_i)^2}, \quad (6)$$

$$BIAS = n^{-1}\sum_{i=1}^{n}(M_i - ref_i), \quad (7)$$

$$ubRMSD = \sqrt{RMSD^2 - BIAS^2}, \quad (8)$$

where n represents the sample size; M_i and ref_i respectively represents multiple sets of reanalysis ET data and reference data at time i. $\bar{M}$ and $\overline{ref}$ represent the average of M_i and ref_i.

3 Results and Discussion

The consistency of the three data sets has been illustrated in Fig. 2, where Fig. 2a-c shows the differences of land evaporation between each data set and ensemble mean. In the high latitudes of the northern hemisphere, GLDAS-Noah2 ET is more than 20% higher than ensemble mean, while ERA5 ET is almost the same with it, even MERRA2 ET more than 20% lower. In the middle latitudes, ERA5 ET is more than 20% higher than ensemble mean, while GLDAS-Noah2 ET is more than 20% lower than it. As for MERRA2 ET, there are a few areas higher than ensemble mean. In the western part of South America and parts of Oceania in the southern hemisphere, ERA5 ET is higher than ensemble mean while GLDAS-Noah2 is lower than it, MERRA2 showing no significant difference. In these regions, the three data sets are significantly different, indicating that the estimation of land evaporation is of great uncertainty and low consistency. In order to reduce the risk of

https://doi.org/10.5194/essd-2021-61
Preprint. Discussion started: 16 March 2021

land evaporation merging, CV is used to select regions with high consistency. Not surprisingly, in the north of North America, west of South America, desert regions of mid-latitude Africa and Asia, CV is above 0.8, indicating relatively low consistency and high risk, thus these regions are excluded from the merging region.

https://doi.org/10.5194/essd-2021-61
Preprint. Discussion started: 16 March 2021

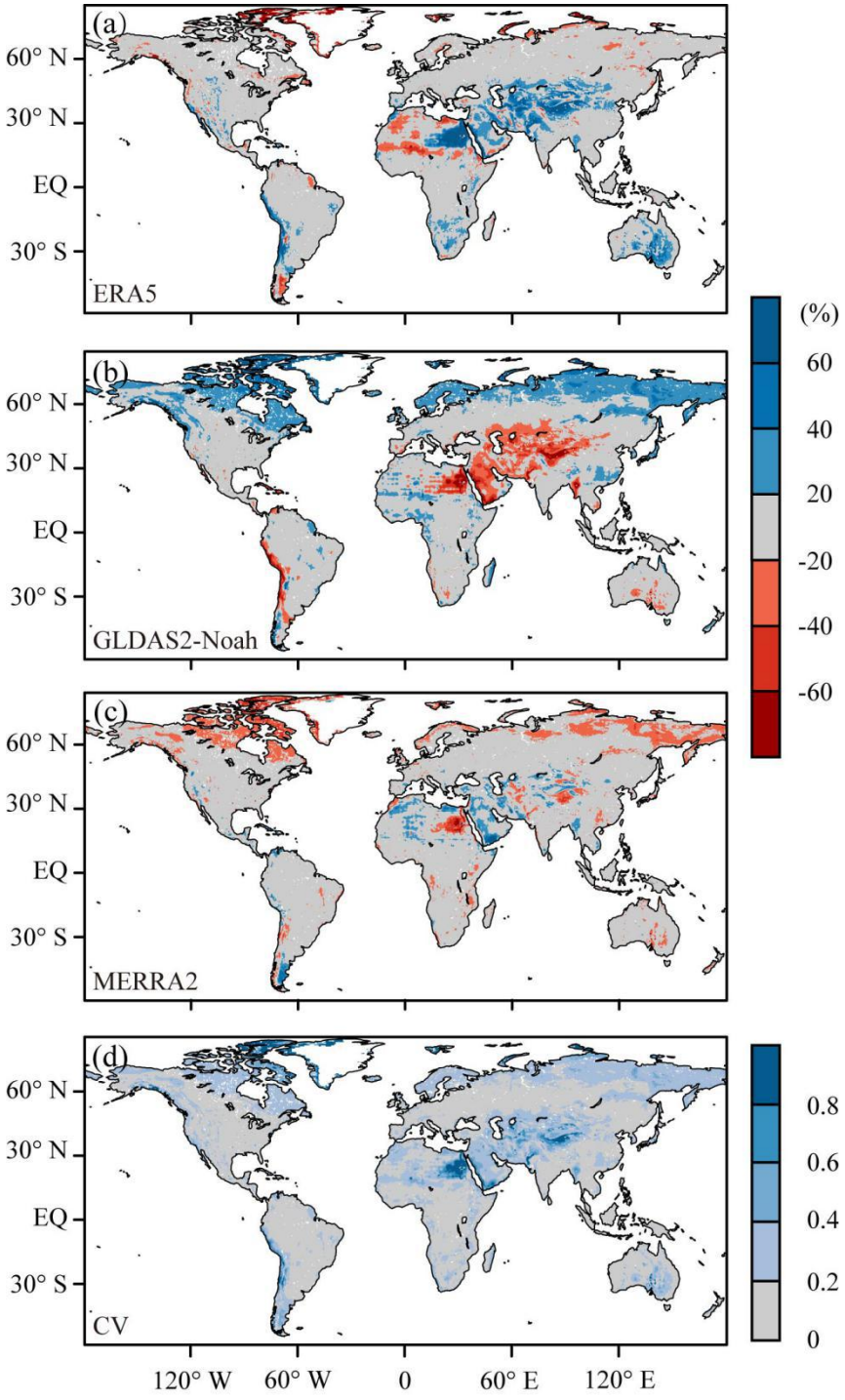

Figure 2. a-c) The percentage of the difference between ERA5, GLDAS2-Noah, MERRA2 and average of the three data sets, d) Variable Coefficient of the three data sets.

https://doi.org/10.5194/essd-2021-61
Preprint. Discussion started: 16 March 2021

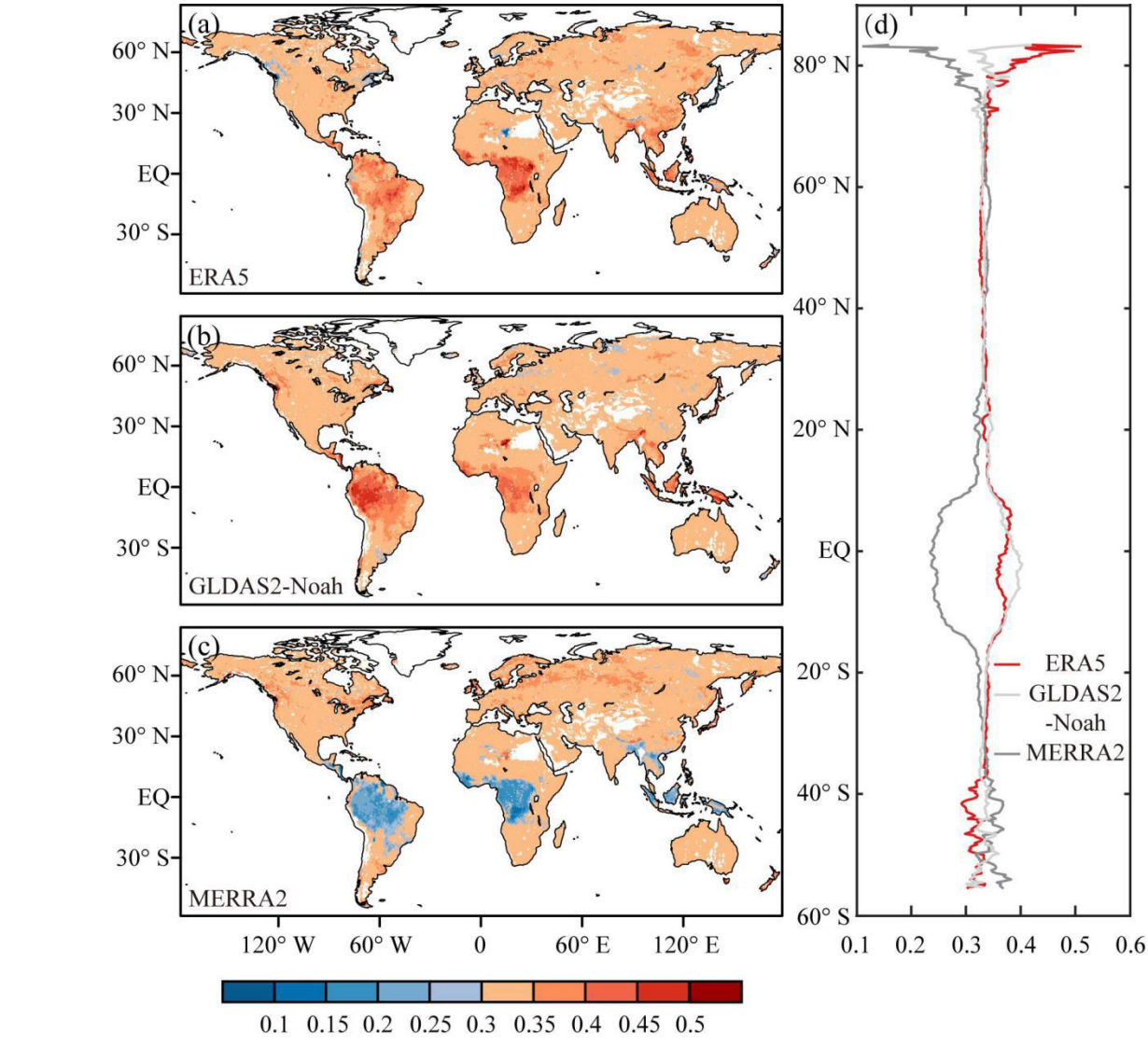

Figure 3. a-c) Spatial distribution of weights, and d) latitudinal distribution of weights.

The spatial distribution of weights has been depicted in Fig. 3, representing the contribution of each data set to the merged product. It is not difficult to find that the weights are within the scope of 0.3 ~ 0.35 in most regions, indicating that the contributions of the three data sets in these regions are basically the same. In the Amazon Plain near the equator, the Congo Basin and the border between Oceania and Asia, the weights of multiple data sets varied greatly. The weights of MERRA2 ET in these regions are below 0.3, while ERA5 ET and GLDAS-Noah2 ET are above 0.35, indicating that MERRA2 ET contributed less than the other two data sets in these regions. GLDAS-Noah2 ET was found to contribute greatly to the Amazon Plain and the border between Oceania and Asia, while in the Congo Basin ERA5 contributed the most. Zonal banded weights of the three data sets are presented in Fig. 3a-c, with the zonal averaged weights. Three curves have been

https://doi.org/10.5194/essd-2021-61
Preprint. Discussion started: 16 March 2021

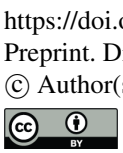

shown in Fig. 3d, which describe the contributions of each data set at different latitudes. Obviously, the contribution of MERRA2 ET is less than that of the other two data sets near the equator, further GLDAS-Noah2 ET contributes slightly more than ERA5 ET. In the high latitudes of the Northern Hemisphere, the difference in contributions among the three data sets is greatest, where the contribution of ERA5 ET is the highest. In the Southern Hemisphere, south of 40S, MERRA2 made a higher contribution than the other two data sets, with little difference in the contribution of the three data sets in other regions.

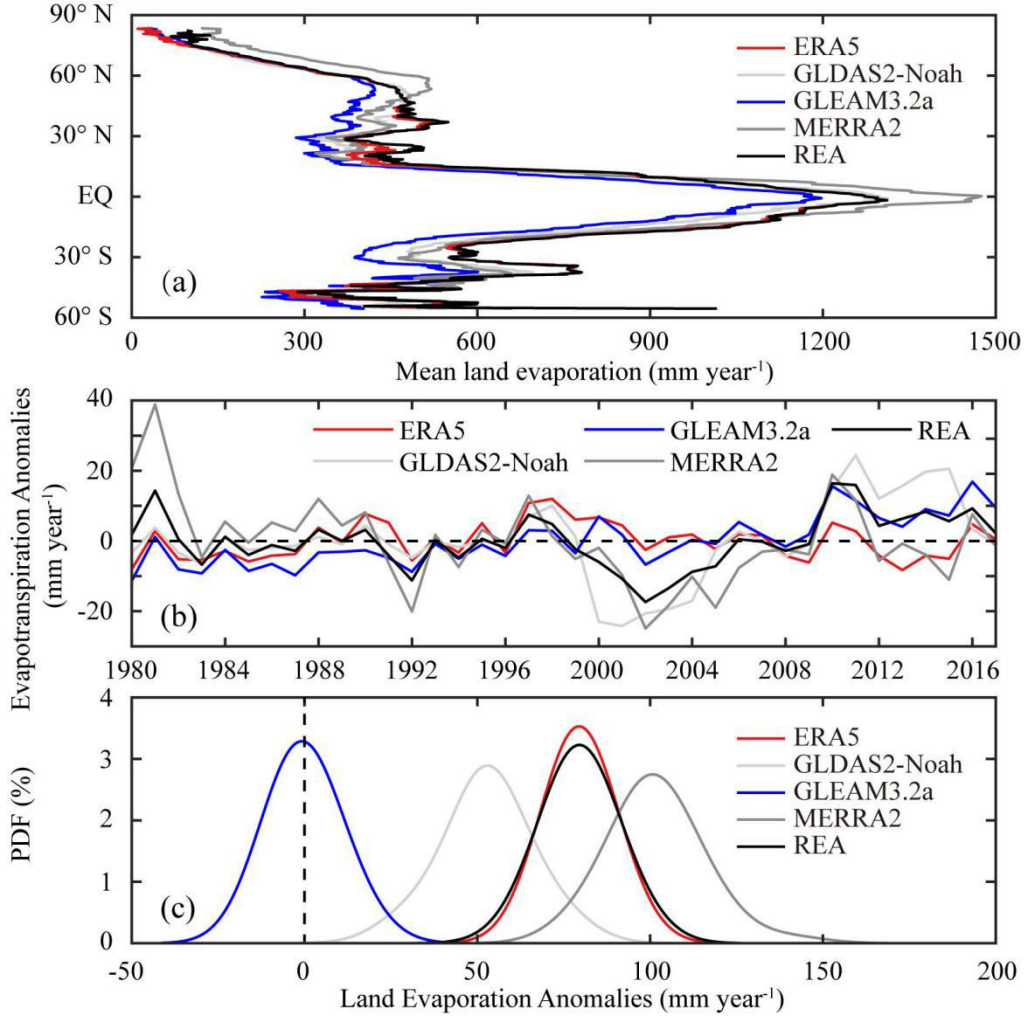

Figure 4. a) Latitudinal distribution of mean land evaporation from five data sets, b) time series (1980-2016), and c) probability distribution of annual land evaporation anomalies from five ET products based on the climatology of GLEAM.

The latitudinal distribution of the multiyear mean land evaporation of five products is shown in Fig. 4a. General consistency in spatial pattern was shown in spite of differences in intensity. However, large differences appeared in the interannual variation of these products (Fig. 4b), though the long-term trends generally showed good consistency. Anomalies for all data

https://doi.org/10.5194/essd-2021-61
Preprint. Discussion started: 16 March 2021

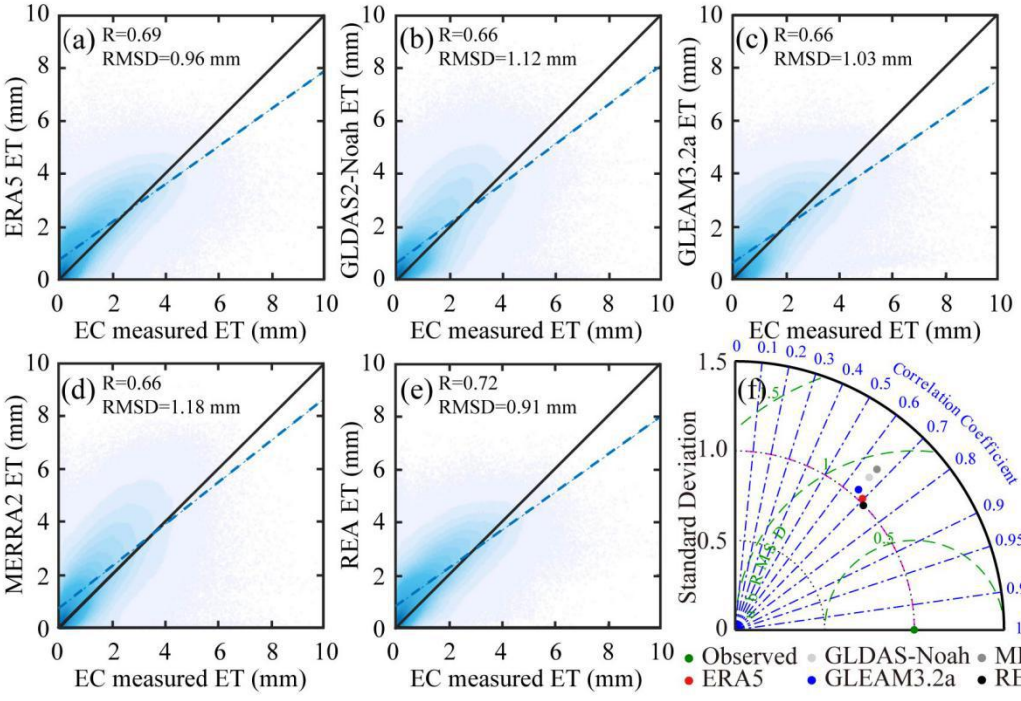

Figure 5. a-e) Scatter plots and f) Taylor diagrams of daily Ground-measure ET and ET from the different products. Linear fits are plotted in blue and the 1:1 line is depicted.

Figure 5a-e shows the scatter diagram of multiple data sets and station-observed data at daily scale. Relatively more points were found to be concentrated above the 1:1 line, which makes it clear that land evaporation was somewhat overestimated. Among the five data sets, the correlation coefficient between REA and station-observed data was the highest, reaching 0.72, followed by ERA5, other three data sets were basically the same. Therefore, the correlation coefficient was significantly improved through REA data merging, indicating more consistent changes between REA and station-observed data. Similarly, as for RMSD, REA was the smallest, only 0.91 mm. Therefore, the deviation between REA data merging product and

https://doi.org/10.5194/essd-2021-61
Preprint. Discussion started: 16 March 2021

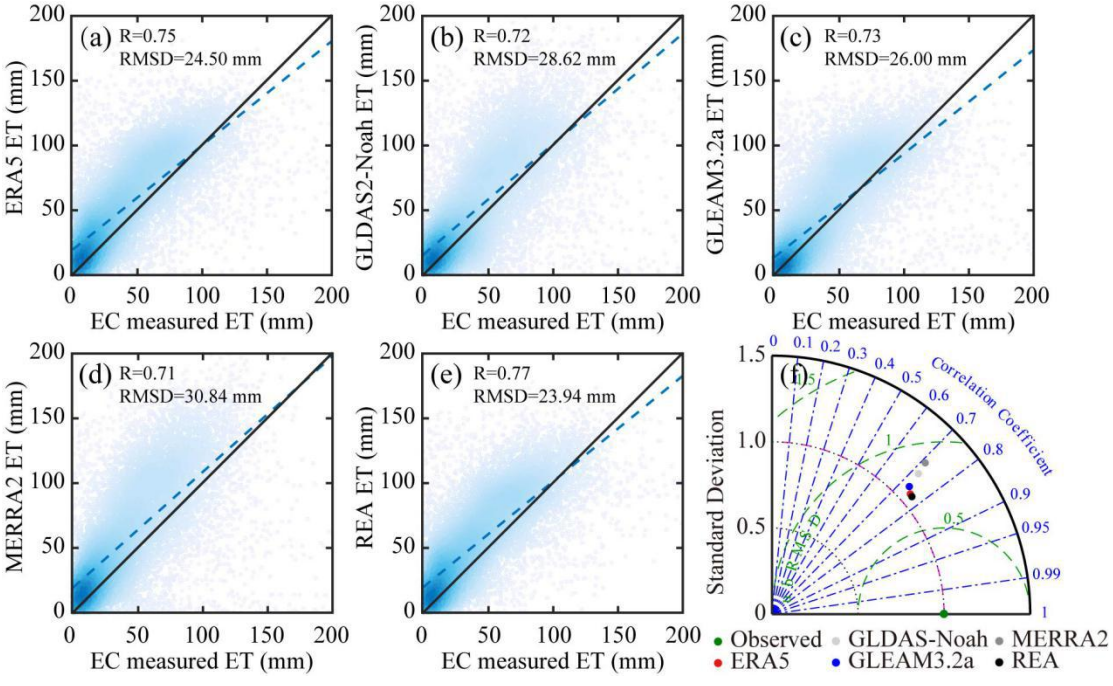

Figure 6. a-e) Scatter plots and f) Taylor diagrams of monthly Ground-measure ET and ET from the different products. Linear fits are plotted in blue and the 1:1 line is depicted.

station-observed data was significantly reduced compared with other data, indicating that the accuracy was greatly improved. The Taylor chart in Fig. 5f describes the ratio of standard deviation, correlation coefficient and unbiased root-mean-square deviation between five data sets and station-observed data under daily scale, with the ratio of standard deviation representing the ratio between each data set and station-observed data. The ratio of standard deviation of REA was the smallest, nearly 1, indicating almost the same with station-observed data and the smallest fluctuation among all data sets considered. The ubRMSD values of multiple data sets were slightly smaller than RMSD respectively, while the rank of them remains the same, specifically REA < ERA5 < GLEAM3.2a < GLDAS-Noah2 < MERRA2. The correlation coefficient between REA and station-observed data was the highest, meanwhile the ratio of standard deviation, RMSD and ubRMSD are the lowest, indicating that REA performed optimally under all assessment criteria.

Figure 6 verifies the quality of multiple land evaporation data sets at monthly scale based on station-observed data. The correlation coefficient between these data sets and station-observed data under monthly scale was higher than that under daily scale, with REA the highest, reaching 0.77. Among the five data sets, RMSD between REA and station-observed data was the smallest, only 23.94 mm. It can be seen from the Taylor chart that the ratio of standard deviation of each data set under monthly scale was larger than that under daily scale, indicating the increase of fluctuation. As with the daily scale, REA performed optimally under all assessment criteria.

https://doi.org/10.5194/essd-2021-61
Preprint. Discussion started: 16 March 2021

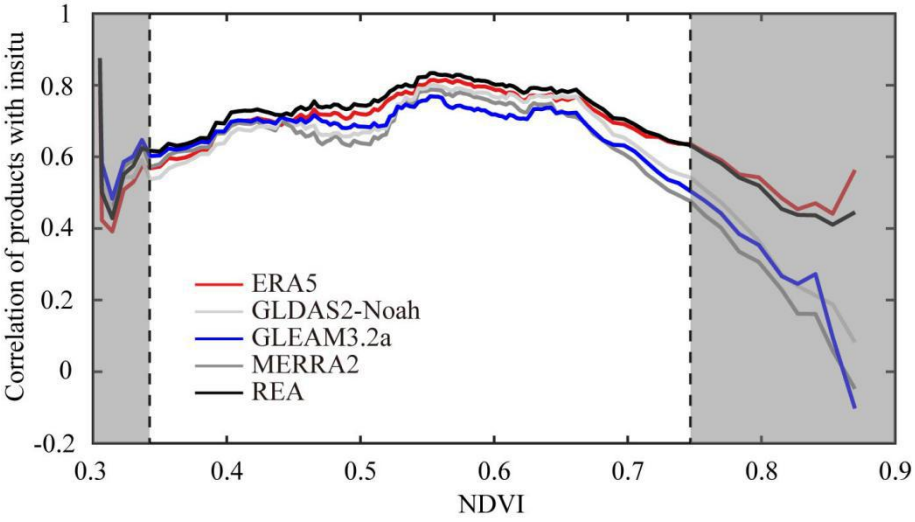

Figure 7. Evaluation over different vegetation densities (NDVI) of the merged product based the correlation coefficient with station-observed data.

Previous studies showed that there is a close relationship between the quality of land evaporation data sets and vegetation (Miralles et al., 2016). The correlation coefficients between multiple data sets and station-observed data under different vegetation conditions (0.3 to 0.9) were compared in order to understand how the quality of these data sets changes with vegetation. The results showed that the quality of all data sets first increased and then decreased with the increase of vegetation density, with the highest quality captured when NDVI was around 0.55. It is worth noting that all data sets were in a good quality range with a correlation of more than 0.6 when NDVI was between 0.4 and 0.7. When NDVI was greater than 0.7, the case of very humid conditions, the quality of each data set was relatively low and showed a rapid decline with the increase of vegetation density. The merged product demonstrated the ability to capture land evaporation dynamics in a wide range of vegetation densities, which performed best in all data sets when NDVI ranges from 0.34 to 0.75.

There are unique advantages and limitations of the existing land ET data sets for specific land cover types, however, quite few are globally suitable for meteorology and hydrology. In different climatic regions, the performance of land ET products varies from the model response. Feng et al. (2018) analyzed correlation between land ET estimated based on the Budyko hypothesis and reanalysis ET products, with results showing that great problems existed in MERRA2 when describing annual variation and long-term trend of land ET in China, mainly due to the higher variance amplitude of MERRA2 than that of other reanalysis products. Further, great uncertainty has been captured in semiarid, semihumid and humid regions according to MERRA2. However, Dembele et al. (2020) found that MERRA2 was still one of the best data sets in estimating land ET in Volta River basin from 2003 to 2012 despite its low spatial resolution, which is probably due to the high temporal but low spatial resolution. In contrast, ERA5 ET behaved poorly in the region. Baik et al. (2018) studied the uncertainty of four widely used ET products (GLDAS2, GLEAM, MOD16 and MERRA) in the dry continent Australia during 2005-2014, finding a good consistency of GLDAS2 in arable land. GLEAM performed well in forest and savanna, while GLDAS2

https://doi.org/10.5194/essd-2021-61
Preprint. Discussion started: 16 March 2021

showed the highest correlation in farmland, grassland, and shrub. However, GLDAS2 and GLEAM ET were found overestimated in most climatic regions and land cover classifications. The difference between model input variables can effectively explain the difference between estimated ET (Yao et al., 2017b). Specifically for Amazon tropical forests, MERRA2 tends to overestimate daily net radiation and incident solar radiation, while GLDAS2 tends to overestimate daily radiation and underestimate incident solar radiation (Gomis-Cebolla et al., 2019).

In our study, GLEAM showed high performance due to the information of soil moisture integrated in the calculation of land ET, which is expected to perform well in the hydrological simulation. Khan et al. (2020) compared multiple sets of ET data sets in different terrains in Australia during 2009-2011, finding that GLEAM was better than GLDAS2. Specifically, GLDAS2 had the best performance in grassland, while GLEAM was very good in forest and grassland. In China, Yang et al. (2017) verified daily GLEAM ET data in different land cover types during 2003-2005 by using China flux tower measurements, with results indicating that GLEAM performed better in grassland ecosystem than forest and farmland. Khan et al. (2018) first applied the extended triple collocation (TC) method to provide unrelated absolute and relative error structures between three available land ET (MOD16, GLEAM, and GLDAS2) products, finding that GLEAM always performed better in forests and GLDAS2 is almost similar to GLEAM in paddy fields and grasslands in the case of minimum absolute and relative uncertainty. Interestingly, the relative uncertainty of all data sets for low vegetation is larger than high canopy.

https://doi.org/10.5194/essd-2021-61
Preprint. Discussion started: 16 March 2021

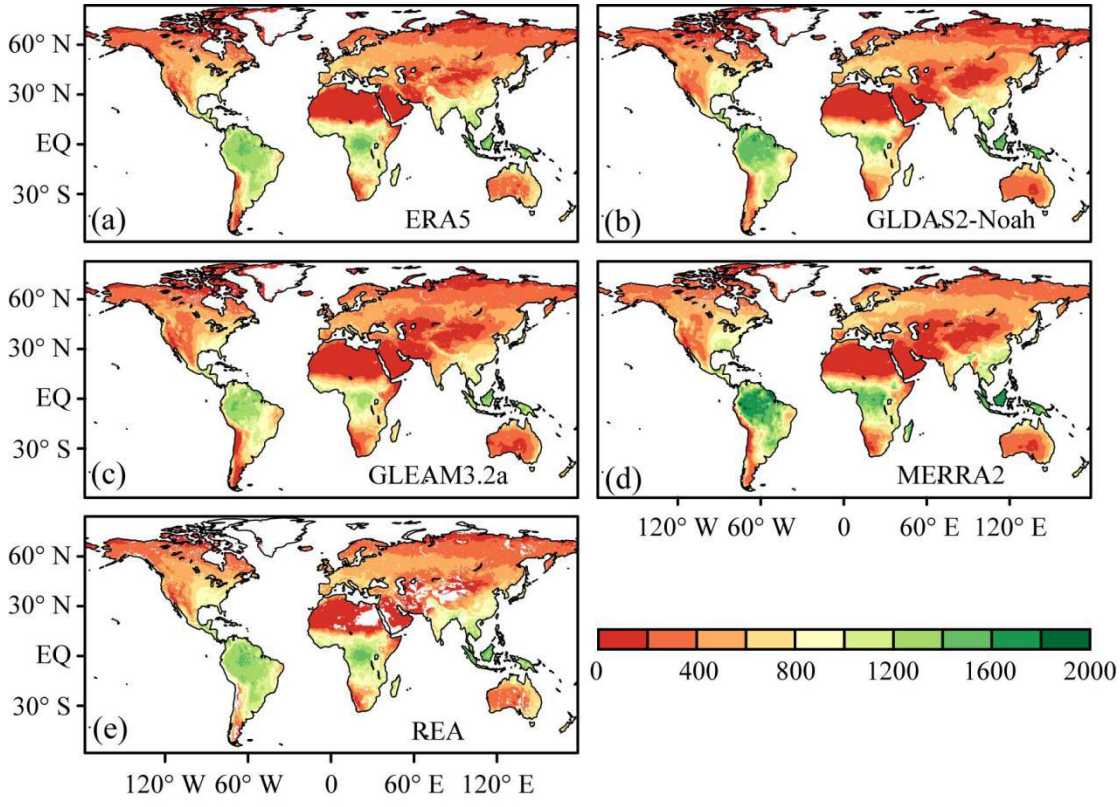

Figure 8. Spatial distribution of annual mean land evaporation for the period 1980-2017 (unit: mm).

Figure 8 depicts the spatial distribution of annual land evaporation, which seems to be relatively consistent of the five data sets. The regions with high land evaporation were found concentrated near the equator, generally very wet regions, including the Amazon Plain in the north of South America, the Congo Basin in central Africa and the border between Asia and Oceania. The rainfall is usually over 1000 mm per year. Extremely low land evaporation was found concentrated in very dry desert and permafrost regions, including the Sahara and Arabian deserts in the north of Africa, the Taklimakan, Turkish, Iranian and Indian deserts in central Asia, and the permafrost regions in the north of North America and Eurasia. The rainfall in dry regions was under 200 mm per year. In comparison with REA, the measurement of MERRA2 and GLDAS-Noah2 was found significantly higher in the very wet regions near the equator, and basically the same in other regions, while GLEAM3.2a was slightly lower in the very wet equatorial regions and significantly lower in the very dry regions of central Asia and the west of North America. The spatial distribution of ERA5 and REA was found to be the most consistent.

https://doi.org/10.5194/essd-2021-61
Preprint. Discussion started: 16 March 2021

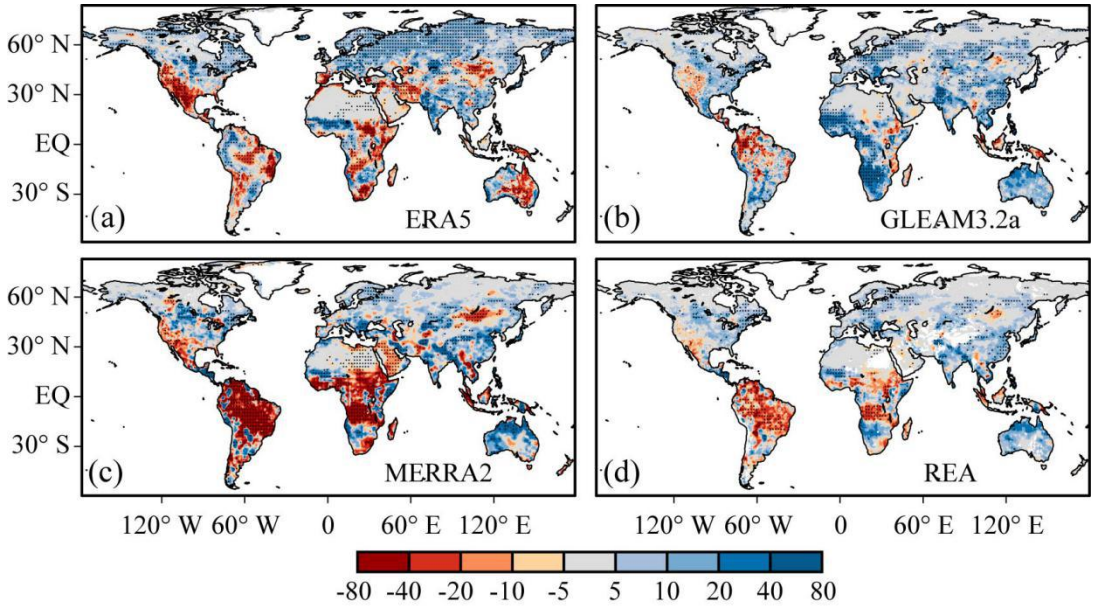

Figure 9. Spatial distribution of linear trends of land evaporation for the period 1980-2017 (unit: mm decade-1). Stippling indicates statistically significant regions at 95% confidence level of the Mann-Kendall test.

Figure 9 depicts the variation trends of multiple data sets during 1980-2017, where GLDAS-Noah2 has not been taken into account due to two data sets including GlDAS-NOah2.0 and Gldas-Noah2.1 used throughout the period. Merged products showed that land evaporation significantly decreased in Amazon Plain in South America and Congo Basin in central Africa, while increased almost all over the world covering the east of North America, west of Europe, south of Asia and north of Oceania. The reduction trend in Amazon has been observed in all data sets, with MERRA2 showing the most significant and intense one. The decreasing trend in the Congo basin was detected in ERA5 and MERRA2, while an opposite one was observed in GLEAM3.2a. Burnett et al. (2020) found Congo basin becoming sunnier and less humid in recent years through the analysis of environmental data. In general, GLEAM is fairly close to land ET in tropical Africa (Schuttemeyer et al., 2007; Opoku-Duah et al., 2008; Andam-Akorful et al., 2015; Liu et al., 2016), while MERRA2 ET had the maximum temporal variability over Congo basin (Burnett et al., 2020; Crowhurst et al., 2020). The increase in the east of North America, west of Europe and south of Asia were detectable in all data sets. The increasing trend in the north of Oceania was also detected in GLEAM3.2a and MERRA2, but not in ERA5.

Varying degrees of uncertainties exist in models based on satellites according to their theories, structural assumption and parameterization of the inputs. These limitations are mainly affected by changes in landscape, climatic and hydrological conditions (Xu et al., 2015). Changes in environmental conditions and extensive vegetation types in regional and global ET estimation can lead to great uncertainties in ET products (Yilmaz et al., 2012; Liaqat and Choi, 2015; Liaqat et al., 2015; Khan et al., 2018). Apart from a few ET products, at present, the validation and analysis have been rarely adopted to reduce uncertainties. A few researches have made some attempts to reduce the uncertainties in hydrological applications

https://doi.org/10.5194/essd-2021-61
Preprint. Discussion started: 16 March 2021

(Zhu et al., 2016), so far no such performance has been achieved yet. An emerging new technology REA method, which has ability to combine different ET products (GLDAS, GLEAM, ERA5 and MERRA2) and is becoming increasingly successful to resolve the issue of hydrological uncertainties and holds greater significance for in-depth assessment.

The uncertainties during the merging of ET products are driven by various factors including input errors, scaling effect and merging algorithm. Input errors are derived from single ET product and EC ground measurements. EC ground measurement determines the accuracy of the merged ET products, as it is considered to be the "true" value used to calibrate single product, which persists an error of about 5-20%. They are usually found relatively accurate for ET acquisition (Foken et al., 2006). The uncertainties from scaling effects are caused by the mismatch between the spatial resolution of the model and the tower footprint. The uncertainties of merging algorithms are caused by differential calculations of the weight of each product. In addition, there are other factors that lead to uncertainties. For example, uncertainties in remote sensing and meteorological data may affect the calculation of modeled ET. With regard to the model estimation, some common modeling assumptions such as estimation of potential evaporation, and shared inputs such as surface radiation make ET estimates from models quite dependent, making the predicted errors correlated (Jimenez et al., 2017).

In general, reasonable information about hydrological variables on a global scale can be extracted from satellite- and reanalysis-based data sets, which is useful in regions lacking sufficient observations (Kim et al., 2018). For the performances of reanalysis and satellite data are discrepant under different mechanisms, the merging method can be used to verify the complementary strategy well to reflect the strengths of both. However, the complex structure of these merging methods affects the efficiency of calculating the weight and limits their wider application. In contrast, the simplicity, computational efficiencies and reliable accuracy of REA method make it more preponderant when considering multi-source data sets (Giorgi & Mearns, 2002). On the basis of previous studies, this study focuses on the global performance of land ET merged product. To reduce the complexity, we introduced REA method to improve land ET estimation and use it as benchmark by merging three reanalysis data sets produced by separate algorithms. This method considers not only the performance of single model, but also the convergence of models involved in the merging process. Compared with a single product, REA merged ET products were found to outperform with significantly reduced root mean square error (RMSE = 0.05~ 0.27mm per day on average) by. However, these merging methods only take into consideration the combination and relationship between each product and the reference data set. Although they are statistically significant, data sets both participating in the merging process and used as reference have not been improved substantially. Therefore, the performance of REA method is highly dependent on the weight of individual data set, which are calibrated with reference data. Future research needs to determine the physical mechanism of the inherent error of each product and strengthen the global quantification of ET products by combining the surface residual energy balance and water balance method without using any reference data set (Yao et al., 2017b; Baik et al., 2018).

https://doi.org/10.5194/essd-2021-61
Preprint. Discussion started: 16 March 2021

4 Data availability

All data used in this study are freely available with the links given in section 2. A convenience copy of the merged global land evaporation product available at the time this paper was created has been registered with Zenodo and is available at https://doi.org/10.5281/zenodo.4595941 (Lu et al., 2021). Both daily and monthly dataset are provided.

5 Conclusion

In conclusion, we used CV as the indicator to select the merging regions with high data consistency, and the regions with low consistency were excluded from the merging scope, including the north of North America, west of South America, desert regions of mid-latitude Africa and Asia. We merged three land ET data sets, ERA5, GLDAS and MERRA2, respectively using REA method to generate a set of long sequence global daily ET data with a spatial resolution of 0.5 degree and a time span of 38 years. The quality of the merged product was found significantly improved when compared with the three individual data sets selected for merging. Both the correlation coefficient and RMSE results suggested that under different vegetation conditions, the quality of the merged product outperformed well among all data sets.

The spatial distribution of the merged product was found highly consistent with other four data sets, indicating that the product successfully captures the spatial difference of land ET effectively. In terms of variation trends of global land ET, conclusions differ from numerous researches due to uncertainties of data used, and no agreement could be reached. Our merged product shows that there is a significant decreasing trend in Amazon plain in South America and Congo Basin in central Africa, and an increasing trend in the east of North America, west of Europe, south of Asia and north of Oceania. This is the first time we have used REA method more precisely in land ET data merging by avoiding the likely errors to be generated by physical mechanism.

Based on model weighting, the method of combining information into a new data set reflects the uncertainty behind climate change predictions, which should be explored in depth. A simple and flexible framework is provided for the exploration according to REA method. As we expected, the error expectation was non-stationary. The weight of each day can be estimated by running a time window centered on the day for making the weight change over time. Shorter time windows produce more dynamic weights, nonetheless, the values may be noisier due to fewer samples available to estimate variability in the time series. Under the framework, cross-variable merging can be realized, that is, multiple related variables can be included for weight calculation (Xu et al., 2010). In future studies, the quality of merged products could be improved by adopting an appropriate time window to calculate the dynamic weight and considering more relevant variables to further reduce the uncertainty of the merged product.

Author contributions. JL conducted the research, completed the original draft, and revised it. TC, SL and DFTH contributed to data processing. GK, JP, TJ and BS revised the draft. GW, the corresponding author, contributed to conceptual

designing, reviewing of the manuscript, funding acquisition, and project administration. All coauthors reviewed the manuscript and contributed to the writing process.

Competing interests. The authors declare that they have no conflict of interest.

Acknowledgments. This study is supported by National Key Research and Development Program of China (2017YFA0603701) and National Natural Science Foundation of China (41875094).

References

Aires, F.: Combining Datasets of Satellite-Retrieved Products. Part I: Methodology and Water Budget Closure, J. Hydrometeorol., 15, 1677-1691, https://doi.org/10.1175/JHM-D-13-0148.1, 2014.

Albergel, C., Dutra, E., Munier, S., Calvet, J.-C., Munoz-Sabater, J., de Rosnay, P., and Balsamo, G.: ERA-5 and ERA-Interim driven ISBA land surface model simulations: which one performs better? Hydrol. Earth Syst. Sc., 22, 3515-3532, https://doi.org/10.5194/hess-22-3515-2018, 2018.

Andam-Akorful, S. A., Ferreira, V. G., Awange, J. L., Forootan, E., and He, X. F.: Multi-model and multi-sensor estimations of evapotranspiration over the Volta Basin, West Africa, Int. J. Climatol., 35, 3132-3145, https://doi.org/10.1002/joc.4198, 2015.

Baik, J., Park, J., Ryu, D., and Choi, M.: Geospatial blending to improve spatial mapping of precipitation with high spatial resolution by merging satellite-based and ground-based data, Hydrol. Process., 30, 2789-2803, https://doi.org/10.1002/hyp.10786, 2016.

Baik, J., Liaqat, U. W., and Choi, M.: Assessment of satellite- and reanalysis-based evapotranspiration products with two blending approaches over the complex landscapes and climates of Australia, Agr. Forest Meteorol., 263, 388-398, https://doi.org/10.1016/j.agrformet.2018.09.007, 2018.

Bosilovich, M. G., Akella, S., Coy, L., Cullather, R., Draper, C., Gelaro, R., Kovach, R., Liu, Q., Molod, A., Norris, P., Wargan, K., Chao, W., Reichle, R., Takacs, L., Vikhliaev, Y., Bloom, S., Collow, A., Firth, S., Labow, G., Partyka, G., Pawson, S., Reale, O., Schubert, S. D., and Suarez, M.: MERRA-2: Initial evaluation of the climate, Technical Report Series on Global Modeling and Data Assimilation, 43,136, 2015.

Burnett, M. W., Quetin, G. R., and Konings, A. G.: Data-driven estimates of evapotranspiration and its controls in the Congo Basin, Hydrol. Earth Syst. Sc., 24, 4189-4211, https://doi.org/10.5194/hess-24-4189-2020, 2020.

Cheema, M. J. M., and Bastiaanssen, W. G. M.: Local calibration of remotely sensed rainfall from the TRMM satellite for different periods and spatial scales in the Indus Basin, Int. J. Remote Sens., 33, 2603-2627, https://doi.org/10.1080/01431161.2011.617397, 2012.

Crowhurst, D., Dadson, S., Peng, J., and Washington, R.: Contrasting controls on Congo Basin evaporation at the two rainfall peaks, Clim. Dynam., https://doi.org/10.1007/s00382-020-05547-1, 2020.

https://doi.org/10.5194/essd-2021-61
Preprint. Discussion started: 16 March 2021

Dembelea, M., Ceperley, N., Zwart, S. J., Salvadore, E., Mariethoz, G., and Schaefl, B.: Potential of satellite and reanalysis evaporation datasets for hydrological modelling under various model calibration strategies, Adv. Water Resour., 143, 103667, https://doi.org/10.1016/j.advwatres.2020.103667, 2020.

Duan, Z., and Bastiaanssen, W.G.M.: First results from Version 7 TRMM 3B43 precipitation product in combination with a new downscaling-calibration procedure. Remote Sens. Environ., 131, 1-13, https://doi.org/10.1016/j.rse.2012.12.002, 2013.

Ershadi, A., McCabe, M. F., Evans, J. P., Chaney, N. W., and Wood, E. F.: Multi-site evaluation of terrestrial evaporation models using FLUXNET data, Agr. Forest Meteorol., 187, 46-61, https://doi.org/10.1016/j.agrformet.2013.11.008, 2014.

Feng, F., Li, X., Yao, Y., Liang, S., Chen, J., Zhao, X., Jia, K., Pinter, K., and McCaughey, J. H.: An empirical orthogonal function-based algorithm for estimating terrestrial latent heat flux from eddy covariance, meteorological and satellite observations, PloS ONE, 11, 1-16, https://doi.org/10.1371/journal.pone.0160150, 2016.

Feng, T., Su, T., Ji, F., Zhi, R., and Han, Z.: Temporal characteristics of actual evapotranspiration over China under global warming, J. Geophys. Res-Atmos., 123, 5845-5858, https://doi.org/10.1029/ 2017JD028227, 2018.

Foken, T., Wimmer, F., Mauder, M., Thomas, C., and Liebethal, C.: Some aspects of the energy balance closure problem, Atmos. Chem. Phys., 6, 4395-4402, https://doi.org/10.5194/acp-6-4395-2006, 2006.

Gelaro, R., McCarty, W., Suárez, M. J., Todling, R., Molod, A., Takacs, L., Randles, C. A., Darmenov, A., Bosilovich, M. G., Reichle, R., Wargan, K., Coy, L., Cullather, R., Draper, C., Akella, S., Buchard, V., Conaty, A., da Silva, A. M., Gu, W., and Kim, G.-K.: The modern-era retrospective analysis for research and applications, version 2 (MERRA-2), J. Climate., 30, 5419-5454, https://doi.org/10.1175/JCLI-D-16-0758.1, 2017.

Giorgi, F., and Mearns, L. O.: Calculation of average, uncertainty range, and reliability of regional climate changes from AOGCM simulations via the "reliability ensemble averaging" (REA) method, J. Climate., 15,1141-1158, https://doi.org/10.1175/1520-0442(2002)015<1141:COAURA>2.0.CO;2, 2002.

Gomis-Cebollaa, J., Jimeneza, J. C., Sobrinoa, J. A., Corbarib, C., and Mancini, M.: Intercomparison of remote-sensing based evapotranspiration algorithms over amazonian forests, Int. J. Appl. Earth Obs., 80, 280-294, https://doi.org/10.1016/j.jag.2019.04.009, 2019.

Hersbach, H., Bell, B., Berrisford, P., Hirahara, S., Horányi, A., Muñoz-Sabater, J., Nicolas, J., Peubey, C., Radu, R., Schepers, D., Simmons, A., Soci, C., Abdalla, S., Abellan, X., Balsamo, G., Bechtold, P., Biavati, G., Bidlot, J., Bonavita, M., Chiara, G., Dahlgren, P., Dee, D., Diamantakis, M., Dragani, R., Flemming, J., Forbes, R., Fuentes, M., Geer, A., Haimberger, L., Healy, S., Hogan, J. R., Hólm, E., Janisková, M., Keeley, S., Laloyaux, P., Lopez, P., Lupu, C., Radnoti, G., Rosnay, de P., Rozum, I., Vamborg, F., Villaume, S., and Thépaut, J.-N.: The ERA5 global reanalysis, Q. J. Roy. Meteor. Soc., 146, 1999-2049, https://dx.doi.org/10.1002/qj.3803, 2020.

Hirschi, M., Seneviratne, S. I., Alexandrov, V., Boberg, F., Boroneant, C., Christensen, O. B., Formayer, H., Orlowsky, B., and Stepanek, P.: Observational evidence for soil-moisture impact on hot extremes in southeastern Europe, Nat. Geosci., 4, 17-21, https://doi.org/10.1038/NGEO1032, 2011.

https://doi.org/10.5194/essd-2021-61
Preprint. Discussion started: 16 March 2021

Hobeichi, S., Abramowitz, G., Evans, J., and Ukkola, A.: Derived Optimal Linear Combination Evapotranspiration (DOLCE): a global gridded synthesis ET estimate, Hydrol. Earth Syst. Sc., 22, 1317-1336, https://doi.org/10.5194/hess-22-1317-2018, 2018.

Jimenez, C., Martens, B., Miralles, D. M., Fisher, J. B., Beck, H. E., and Fernández-Prieto, D.: Exploring the merging of the global land evaporation WACMOS-ET products based on local tower measurements, Hydrol. Earth Syst. Sc., 22, 4513-4533, https://doi.org/10.5194/hess-22-4513-2018, 2018.

Jimenez, C., Martens, B., Miralles, D. M., Fisher, J. B., Beck, H. E., and Fernández-Prieto, D.: Local tower-based merging of two land evaporation products, Hydrol. Earth Syst. Sci. Discuss., 1-41, https://doi.org/10.5194/hess-2017-573, 2017.

Jimenez, C., Prigent, C., Mueller, B., Seneviratne, S. I., McCabe, M. F., Wood, E. F., Rossow, W. B., Balsamo, G., Betts, A. K., Dirmeyer, P. A., Fisher, J. B., Jung, M., Kanamitsu, M., Reichle, R. H., Reichstein, M., Rodell, M., Sheffield, J., Tu, K., and Wang, K.: Global intercomparison of 12 land surface heat flux estimates, J. Geophys. Res-Atmos., 116, 102-127, https://doi.org/10.1029/2010JD014545, 2011.

Jung, M., Reichstein, M., Ciais, P., Seneviratne, S. I., Sheffield, J., Goulden, M. L., Bonan, G., Cescatti, A., Chen, J. Q., de Jeu, R., Dolman, A. J., Eugster, W., Gerten, D., Gianelle, D., Gobron, N., Heinke, J., Kimball, J., Law, B. E., Montagnani, L., Mu, Q. Z., Mueller, B., Oleson, K., Papale, D., Richardson, A. D., Roupsard, O., Running, S., Tomelleri, E., Viovy, N., Weber, U., Williams, C., Wood, E., Zaehle, S., and Zhang, K.: Recent decline in the global land evapotranspiration trend due to limited moisture supply, Nature, 467, 951-954, https://doi.org/10.1038/nature09396, 2010.

Khan, M. S., Baik, J., and Choi, M.: Inter-comparison of evapotranspiration datasets over heterogeneous landscapes across Australia, Adv. Space Res., 66, 533-545, https://doi.org/10.1016/j.asr.2020.04.037, 2020.

Khan, M. S., Waqas, U., Baik, J., and Choi, M.: Stand-alone uncertainty characterization of GLEAM, GLDAS and MOD16 evapotranspiration products using an extended triple collocation approach, Agr. Forest Meteorol., 252, 256-268, https://doi.org/10.1016/j.agrformet.2018.01.022, 2018.

Kim, H., Parinussa, R., Konings, A. G., Wagner, W., Cosh, M. H., Lakshmi, V., Zohaib, M., and Choi. M.: Global-scale assessment and combination of SMAP with ASCAT (active) and AMSR2 (passive) soil moisture products, Remote Sens. Environ., 204, 260-275, https://doi.org/10.1016/j.rse.2017.10.026, 2018.

Kim, S., Parinussa, R. M., Liu, Y. Y., Johnson, F. M., and Sharma, A.: A framework for combining multiple soil moisture retrievals based on maximizing temporal correlation, Geophys. Res. Lett., 42, 6662-6670, https://doi.org/10.1002/2015GL064981, 2015.

Koster, R. D., Suárez, M. J., Ducharne, A., Stieglitz, M., and Kumar P.: A catchment-based approach to modeling land surface processes in a GCM, Part 1, Model structure, J. Geophys. Res-Atmos., 105, 24809-24822, https://doi.org/10.1029/2000JD900327, 2000.

Liaqat, U. W., and Choi, M.: Surface energy fluxes in the Northeast Asia ecosystem: SEBS and METRIC models using Landsat satellite images. Agr. Forest Meteorol., 214-215, 60-79, https://doi.org/10.1016/j.agrformet.2015.08.245, 2015.

https://doi.org/10.5194/essd-2021-61
Preprint. Discussion started: 16 March 2021

Liaqat, U. W., Choi, M., and Awan, U. K.: Spatio-temporal distribution of actual evapotranspiration in the Indus Basin Irrigation System, Hydrol. Process., 29, 2613-2627, https://doi.org/10.1002/hyp.10401, 2015.

Liu, C., Shu, S., and Gao, W.: Improved sensible and latent heat flux estimation of community land model by using ensemble Kalman filter assimilation, Proc. SPIE, 8869, 886917, https://doi.org/10.1117/12.2021713, 2013.

Liu, W., Wang, L., Zhou, J., Li, Y., Sun, F., Fu, G., Li, X., and Sang, Y. F.: A worldwide evaluation of basin-scale evapotranspiration estimates against the water balance method, J. Hydrol., 538, 82-95, https://doi.org/10.1016/j.jhydrol.2016.04.006, 2016.

Lu, J., Wang, G., Chen, T., Li, S., Hagan, F. T. D., Kattel, G., Peng, J, Jiang, T. and Su, B.: A Harmonized Global Land Evaporation Dataset from Reanalysis Products Covering 1980-2017, Zenodo, https://doi.org/10.5281/zenodo.4595941, 2021.

McCabe, M. F., Ershadi, A., Jimenez, C., Miralles, D. G., Michel, D., and Wood, E. F.: The GEWEX LandFlux project: evaluation of model evaporation using tower-based and globally gridded forcing data, Geosci. Model. Dev., 9, 283-305, https://doi.org/10.5194/gmd-9-283-2016, 2016.

Miralles, D. G., De Jeu, R. A. M., Gash, J. H., Holmes, T. R. H., and Dolman, A. J.: Magnitude and variability of land evaporation and its components at the global scale, Hydrol. Earth Syst. Sc., 15, 967-981, https://doi.org/10.5194/hess-15-967-2011, 2011.

Miralles, D. G., Jiménez, C., Jung, M., Michel, D., Ershadi, A., McCabe, M. F., Hirschi, M., Martens, B., Dolman, A. J., Fisher, J. B., Mu, Q., Seneviratne, S. I., Wood, E. F., Fernández-Prieto, D.: The WACMOS-ET project-part 2: evaluation of global terrestrial evaporation data sets, Hydrol. Earth Syst. Sc., 20, 823-842, https://doi.org/10.5194/hess-20-823-2016, 2016.

Monteith, J. L.: Evaporation and the Environment, Sym. Soc. Exp. Biol., 19, 205-234, 1965.

Mu, Q., Zhao, M., and Steven, W.: Improvements to a MODIS global terrestrial evapotranspiration algorithm, Remote Sens. Environ., 115, 1781-1800, https://doi.org/10.1016/j.rse.2011.02.019, 2011.

Mueller, B., and Seneviratne, S. I.: Hot days induced by precipitation deficits at the global scale, P. Natl. Acad. Sci. USA, 109, 12398- 12403, https://doi.org/10.1073/pnas.1204330109, 2012.

Mueller, B., Hirschi, M., Jimenez, C., Ciais, P., Dirmeyer, P. A., Dolman, A. J., Fisher, J. B., Jung, M., Ludwig, F., Maignan, F., Miralles, D. G., McCabe, M. F., Reichstein, M., Sheffield, J., Wang, K., Wood, E. F., Zhang, Y., and Seneviratne, S. I.: Benchmark products for land evapotranspiration: LandFlux-EVAL multi-data set synthesis, Hydrol. Earth Syst. Sc., 17, 3707-3720, https://doi.org/10.5194/hess-17-3707-2013, 2013.

Mueller, B., Seneviratne, S. I., Jimenez, C., Corti, T., Hirschi, M., Balsamo, G., Ciais, P., Dirmeyer, P., Fisher, J. B., Guo, Z., Jung, M., Maignan, F., McCabe, M. F., Reichle, R., Reichstein, M., Rodell, M., Sheffield, J., Teuling, A. J., Wang, K., Wood, E. F., and Zhang, Y.: Evaluation of global observations-based evapotranspiration datasets and IPCC AR4 simulations, Geophys. Res. Lett., 38, L06402, https://doi.org/10.1029/2010GL046230, 2011.

Munier, S., Aires, F., Schlaffer, S., Prigent, C., Papa, F., Maisongrande, P., and Pan, M.: Combining data sets of satellite-

https://doi.org/10.5194/essd-2021-61
Preprint. Discussion started: 16 March 2021

retrieved products for basin-scale water balance study: 2. Evaluation on the Mississippi Basin and closure correction model, J. Geophys. Res-Atmos., 119, 12100-12116, https://doi.org/10.1002/2014JD021953, 2014.

Opoku-Duah, S., Donoghue, D. N. M., and Burt, T. P.: Intercomparison of evapotranspiration over the Savannah Volta Basin in West Africa using remote sensing data, Sensors, 8, 2736-2761, https://doi.org/10.3390/s8042736, 2008.

Peng, J., Kharbouche, S., Muller J-P., Danne O., Blessing S., Giering R., Gobron N., Ludwig R., Muller B., Leng G., Lees T., Dadson S.: Influences of leaf area index and albedo on estimating energy fluxes with HOLAPS framework, J. Hydrol., 580, 124245, https://doi.org/10.1016/j.jhydrol.2019.124245, 2020.

Peng, J., Loew, A., Chen, X., Ma, Y., and Su, Z.: Comparison of satellite based evapotranspiration estimates over the Tibetan Plateau, Hydrol. Earth Syst. Sc., 20, 3167-3182, https://doi.org/10.5194/hess-20-3167-2016, 2016.

Pipunic, R. C., Walker, J. P., and Western, A. Assimilation of remotely sensed data for improved latent and sensible heat flux prediction: A comparative synthetic study, Remote Sens. Environ., 112,1295-1305, https://doi.org/10.1016/j.rse.2007.02.038, 2008.

Priestley, C. H. B., and Taylor, R. J.: On the assessment of surface heat flux and evaporation using large-scale parameters, Mon. Weather Rev., 100, 81-92, https://doi.org/10.1175/1520-0493(1972)100<0081:OTAOSH>2.3.CO;2, 1972.

Randles, C. A., da Silva, A. M., Buchard, V., Colarco, P. R., Darmenov, A., Govindaraju, R., Smirnov, A., Holben, B., Ferrare, R., Hair, J., Shinozuka, Y., and Flynn, C. J.: The MERRA-2 Aerosol Reanalysis, 1980 Onward. Part I: System Description and Data Assimilation Evaluation, J. Climate, 30, 6823-6850, https://doi.org/10.1175/JCLI-D-16-0609.1, 2017.

Reichle, R. H., Liu, Q., Koster, R. D., Draper, C. S., Mahanama, S. P., and Partyka, G. S.: Land surface precipitation in MERRA-2, J. Climate, 30, 1643-1664, https://doi.org/10.1175/JCLI-D-16-0570.1, 2017.

Rodell, M., Houser, P. R., Jambor, U., Gottschalck, J., Mitchell, K., Meng, C.-J., Arsenault, K., Cosgrove, B., Radakovich, J., Bosilovich, M., Entin, J. K., Walker, J. P., Lohmann, D., and Toll, D.: The Global Land Data Assimilation System, B. Am. Meteorol. Soc., 85, 381-394, https://doi.org/10.1175/ BAMS-85-3-381, 2004.

Schuttemeyer, D., Schillings, C., Moene, A. F., and de Bruin, H. A. R.: Satellite-based actual evapotranspiration over drying semi-arid terrain in West Africa, J. Appl. Meteorol. Clim., 46, 97-111, https://doi.org/10.1175/JAM2444.1, 2007.

Seneviratne, S. I., Corti, T., Davin, E. L., Hirschi, M., Jaeger, E. B., Lehner, I., Orlowsky, B., and Teuling, A. J.: Investigating soil moisture-climate interactions in a changing climate: A review, Earth-Sci. Rev., 99, 125-161, https://doi.org/10.1016/j.earscirev.2010.02.004, 2010.

Seneviratne, S. I., Lüthi, D., Litschi, M., and Schär, C.: Land-atmosphere coupling and climate change in Europe, Nature, 443, 205-209, https://doi.org/10.1038/nature05095, 2006.

Seneviratne, S. I.: Climate science: Historical drought trends revisited, Nature, 491, 338-339, https://doi.org/10.1038/491338a, 2012.

Sheffield, J., and Wood, E. F.: Characteristics of global and regional drought, 1950-2000: Analysis of soil moisture data from off-line simulation of the terrestrial hydrologic cycle, J. Geophys. Res-Atmos., 112, D17115,

https://doi.org/10.5194/essd-2021-61
Preprint. Discussion started: 16 March 2021

https://doi.org/10.1029/2006JD008288, 2007.

595 Sheffield, J., Wood, E. F., and Roderick, M. L.: Little change in global drought over the past 60 years, Nature, 491, 435-438, https://doi.org/10.1038/nature11575, 2012.

Sheffifield, J., Goteti, G., and Wood, E. F.: Development of a 50-year high-resolution global dataset of meteorological forcings for land surface modeling, J. Climate, 19, 3088-3111, https://doi.org/10.1175/JCLI3790.1, 2006.

Wang, W., Cui, W., Wang, X., and Chen, X.: Evaluation of GLDAS-1 and GLDAS-2 forcing data and Noah model
600 simulations over China at the monthly scale, J. Hydrometeorol., 17, 2815-2833, https://doi.org/10.1175/JHM-D-15-0191.1, 2016.

Xu, S., Wu, C., Wang, L., Gonsamo, A., Shen, Y., and Niu, Z.: A new satellite-based monthly precipitation downscaling algorithm with non-stationary relationship between precipitation and land surface characteristics, Remote Sens. Environ., 162, 119-140, https://doi.org/10.1016/j.rse.2015.02.024, 2015.

605 Xu, Y., Gao, X., and Giorgi, F.: Upgrades to the reliability ensemble averaging method for producing probabilistic climate-change projections, Clim. Res., 41, 61-81, https://doi.org/doi: 10.3354/cr00835, 2010.

Yang, X., Yong, B., Ren, L., Zhang, Y., and Long, D.: Multi-scale validation of GLEAM evapotranspiration products over China via China FLUX ET measurements, Int. J. Remote Sens., 38, 5688-5709, https://doi.org/10.1080/01431161.2017.1346400, 2017.

610 Yang, Z., Zhang, Q., Yang, Y., Hao, X., and Zhang, H.: Evaluation of evapotranspiration models over semi-arid and semi-humid areas of China, Hydrol. Process., 30, 4292-4313, https://doi.org/10.1002/hyp.10824, 2016.

Yao, Y., Liang, S., Li, X., Chen, J., Liu, S., Jia, K., Zhang, X., Xiao, Z., Fisher, J. B., Mu, Q., Pan, M., Liu, M., Cheng, J., Jiang, B., Xie, X., Grnwald, T., Bernhofer, C., and Roupsard, O.: Improving global terrestrial evapotranspiration estimation using support vector machine by integrating three process-based algorithms, Agr. Forest Meteorol., 242, 55-
615 74, https://doi.org/10.1016/j.agrformet.2017.04.011, 2017a.

Yao, Y., Liang, S., Li, X., Hong, Y., Fisher, J., Zhang, N., Chen, J., Cheng, J., Zhao, S., Zhang, X., Jiang, B., Sun, L., Jia, K., Wang, K., Chen, Y., Mu, Q., and Feng, F.: Bayesian multimodel estimation of global terrestrial latent heat flux from eddy covariance, meteorological, and satellite observations, J. Geophys. Res-Atmos., 119, 4521-4545, https://doi.org/10.1002/2013JD020864, 2014.

620 Yao, Y., Liang, S., Li, X., Liu, S., Chen, J., Zhang, X., Jia, K., Xie, X., Munier, S., Liu, M., Yu, J., Lindroth, A., Varlagin, A., Raschi, A., Noormets, A., Pio, C., Wohlfahrt, G., Sun, G., Domec, J. C., Montagnani, L., Lund, M., Eddy, M., Blanken, P. D., Grünwald, T., Wolf, S., and Magliulo, V.: Assessment and simulation of global terrestrial latent heat flux by synthesis of CMIP5 climate models and surface eddy covariance observations. Agr. Forest Meteorol., 223, 151-167, https://doi.org/10.1016/j.agrformet.2016.03.016, 2016.

625 Yao, Y., Liang, S., Li, X., Zhang, Y., Chen, J., Jia, K., Zhang, X., Fisher, J., Wang, X., Zhang, L., Xu, J., Shao, C., Posee, G., Li, Y., Magliulo, V., Varlagin, A., Moors, E. J., Boike, J., Macfarlane, C., Kato, T., Buchmann, N., Billesbach, D. P., Berimger, J., Wolf, S., Papuga, S. A., Wohlfahrt, G., Montagnani, L., Ardö, J., Paul-Limoges, E., Emmel, C., Hörtnagl,

https://doi.org/10.5194/essd-2021-61
Preprint. Discussion started: 16 March 2021

L., Sachs, T., Gruening, C., Gioli, B., López-Ballesteros, A., Steinbrecher, R., and Gielen, B.: Estimation of high-resolution terrestrial evapotranspiration from Landsat data using a simple Taylor skill fusion method, J. Hydrol., 553, 508-526, https://doi.org/10.1016/j.jhydrol.2017.08.013, 2017b.

Yilmaz, M. T., Crow, W. T., Anderson, M. C., and Hain, C.: An objective methodology for merging satellite - and model - based soil moisture products, Water Resour. Res., 48, W11502, https://doi.org/10.1029/2011WR011682, 2012.

Zhu, G., Li, X., Zhang, K., Ding, Z., Han, T., Ma, J., Huang, C., He, J., and Ma, T.: Multi model ensemble prediction of terrestrial evapotranspiration across north China using Bayesian model averaging, Hydrol. Process., 30, 2861-2879, https://doi.org/10.1002/hyp.10832, 2016.